Antarct. Meteorite Res., **15**, 78–96, 2002

Minor element chemistry of low-Ca pyroxene in Allan Hills-77252, an L3-6 regolith breccia

Takayuki Tomiyama[1], Akira Yamaguchi[1,2], Keiji Misawa[1,2] and Hideyasu Kojima[1,2]

[1]*Department of Polar Science, School of Mathematics and Physics, The Graduate University for Advanced Studies, Kaga 1-chome, Itabashi-ku, Tokyo 173-8515*
[2]*Antarctic Meteorite Research Center, National Institute of Polar Research, Kaga 1-chome, Itabashi-ku, Tokyo 173-8515*

Abstract: Allan Hills (ALH-) 77252 is a regolith breccia consisting of various types of clasts differing in metamorphic grades (L3-6). Titanium/aluminum ratios of low-Ca pyroxene in ALH-77252 are bimodally distributed. In equilibrated clasts, Ti/Al ratios of low-Ca pyroxene are ~0.5 which are quite different from those in unequilibrated clasts of ~0.07. Among equilibrated and unequilibrated clasts, the Ti/Cr ratio of low-Ca pyroxene also shows large differences. Because titanium and aluminum are not diffusive elements in the pyroxene crystal structure, diffusional redistribution of titanium and aluminum in low-Ca pyroxene requires significantly higher metamorphic temperature than Fe-Mg homogenization, possibly above ~800°C. Alternatively, if the source materials of L-group chondrites were initially different, the fingerprints of mineral properties resistant to thermal metamorphism remain unchanged. If this was the case, the distinctly higher Ti/Al ratios of low-Ca pyroxene in equilibrated clasts originated from the primary signatures of low-Ca pyroxene prior to thermal metamorphism.

1. Introduction

Brecciated ordinary chondrites are ubiquitous and consist of clasts with distinctive lithologies within a single specimen (Binns, 1967; Scott *et al.*, 1985; Rubin, 1990). Regolith breccias of ordinary chondrites consist of light colored fragments of chondritic material in dark clastic material and are enriched in noble gases implanted by solar wind (Wasson, 1974; Keil, 1982; Bunch and Rajan, 1988). They are considered to be formed by lithification of regolith by impact(s) on the surface of the chondrite parent body and are primarily mixtures of chondritic materials of the same chemical group but of different petrologic types (Binns, 1967, 1968; Wasson, 1974; Keil, 1982; Scott, 1984; Bunch and Rajan, 1988). Foreign and/or impact-melted clasts are in some cases included in regolith breccias (Fodor and Keil, 1976; Scott *et al.*, 1981a,b; Rubin *et al.*, 1983; Bischoff *et al.*, 1993). Mixing of a single chemical group of chondritic materials implies that constituents of regolith breccia are mainly derived from a single parent body or from closely related parent bodies.

By analogy with unbrecciated ordinary chondrites, the chemical characteristics of chondritic regolith are obvious in the Fe/(Fe+Mg) ratios of the constituent olivine and low-Ca pyroxene, which vary in unequilibrated ordinary chondrites (UOCs) but are uniform in equilibrated ordinary chondrites (EOCs) (Binns, 1967, 1968; Wasson, 1974;

Keil, 1982; Scott, 1984; Bunch and Rajan, 1988). Minor element contents in low-Ca pyroxene vary significantly in the regolith breccia of the H chondrite, Weston (Noonan and Nelen, 1976). In Weston, low-Ca pyroxenes in unequilibrated chondritic xenoliths are rich in chromium and poor in titanium in comparison with those in recrystallized and equilibrated chondritic inclusions. These variations could reflect the relationship between the mineral chemistries and metamorphic degrees of the different materials. Previous studies showed that minor element compositions in low-Ca pyroxene vary in relation to metamorphic grades (Heyse, 1978; McCoy *et al.*, 1991). Heyse (1978) showed systematic changes in the chromium, aluminum, sodium and titanium abundances in low-Ca pyroxene with increasing wollastonite (Wo) contents, which are correlated with estimated metamorphic temperatures and pressures. On the other hand, McSween and Patchen (1989) could not find any correlation between aluminum and Wo in low-Ca pyroxene. An understanding of minor element behavior in low-Ca pyroxene during thermal metamorphism and brecciation processes will give us information about the evolutional history of chondrite regolith breccias. We thus performed mineralogical and petrological studies on an L3-6 breccia, ALH-77252, mainly focusing on the minor element compositions of low-Ca pyroxene and here we discuss the evolutional history of the chondrite parent body.

2. Sample and experiment

On the basis of its mineralogy and petrology, ALH-77252 was previously classified as L4/L6 (King *et al.*, 1980), L3/L6 (Score *et al.*, 1981), or L3 (Scott, 1984; Yanai and Kojima, 1987). An acid residue fraction of ALH-77252 shows a heavy rare-earth element enriched pattern with a large positive Eu anomaly which is typically observed in EOCs (Ebihara, 1989). Noble gases implanted by solar wind are highly enriched in ALH-77252, suggesting that it is a regolith breccia (Nautiyal *et al.*, 1984; Scott, 1984). ALH-77252 is claimed to be paired with ALH-77215, ALH-77216 and ALH-77217 (King *et al.*, 1980). According to the thermoluminescence sensitivities, Sears *et al.* (1991) assigned petrologic subtype 3.7/3.9 for ALH-77216. ALH-77215 contains graphite-magnetite aggregates that originated from an exotic chondritic source (Scott *et al.*, 1981a, b).

In this study, we examined about 2 cm^2 area of ALH-77252 in three polished thin-sections (PTS ,84-1 ,91-1 and ,91-2). Petrologic observation was performed using an optical microscope and a scanning electron microscope (JEOL JSM-5900) equipped with an energy-dispersive system (Oxford LINK ISIS). The chemical compositions of minerals and glasses were determined by an electron microprobe analyzer (JEOL JXA-8800M) using an accelerating voltage of 15 kV, a beam current of 12 or 30 nA and counting times of 30–120 s for olivine, pyroxene and chromite, and 10–30 s for feldspar, Ca-phosphate and glass. Analyses with the 30 nA beam were used for the minor element chemistry. Typical detection limits (wt%) for 30 nA analyses are as follows: Na_2O, MgO, 0.003; SiO_2, Al_2O_3, 0.005; CaO, 0.006; TiO_2, Cr_2O_3, MnO, FeO, 0.01.

There are five major types of pyroxene in ordinary chondrites: low-Ca clinopyroxene, low-Ca orthopyroxene, pigeonite, subcalcic augite and augites. low-Ca clinopyroxene and low-Ca orthopyroxene ($Wo_{<2}$), which inverted from protoenstatite, are compositionally indistinguishable. In this study, followed by Noguchi (1989), we

classified pyroxene by their Wo contents (low-Ca clino/orthopyroxene, $Wo_{<2}$; orthopyroxene, $Wo_{2\text{-}5}$; pigeonite, $Wo_{5\text{-}15}$; subcalcic-augite, $Wo_{15\text{-}25}$; augite, $Wo_{>25}$).

The shock stages of the clasts were determined using the criteria of Stöffler *et al.* (1991).

3. Results

3.1. Overview

ALH-77252 consists of clasts, such as sub-angular lithic fragments (up to 3.5 mm in size), chondrules, melt rock fragments and mineral fragments (Fig. 1). Fine-grained mineral fragments up to a few tens of μm in size constitute the clastic matrix (Ashworth, 1977). Some olivines show undulatory extinction, planar fractures and mosaicism. Maskelynized feldspar is virtually absent. These features indicate that ALH-77252 is composed of clasts with shock stages up to S4.

The chemical compositions of constituent phases in representative clasts and clastic

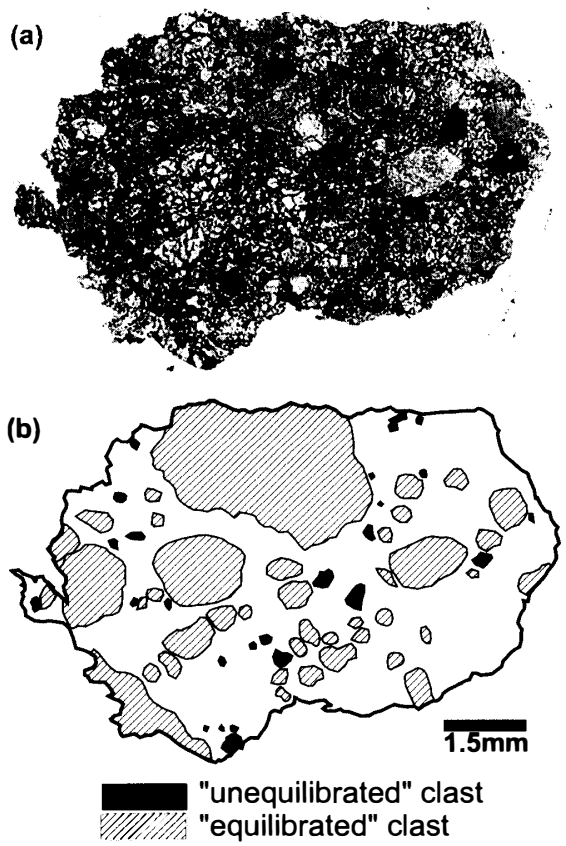

Fig. 1. (a) Photomicrograph of ALH-77252 (PTS ,84-1, plane polarized light). (b) Sketch of identified clasts. Light-hatched areas represent equilibrated clasts, where olivine and low-Ca pyroxene are equilibrated. The 100 Fe/(Fe+Mg) atomic ratios in olivine and in low-Ca pyroxene are within the range of equilibrated L-group chondrites (i.e., $Fa_{22\text{-}25}$, $Fs_{19\text{-}22}$). Dark hatched areas represent unequilibrated clasts, in which the 100 Fe/(Fe+Mg) ratios of olivine and low-Ca pyroxene are variable. The remainder is clastic matrix, which composed of fine-grained mineral fragments up to a few tens of μm in size.

Table 1. Average compositions (wt%) of constituent phases in representative clasts and clastic matrix.

clast	phase	n	Na2O	MgO	Al2O3	SiO2	P2O5	K2O	CaO	TiO2	V2O3	Cr2O3	MnO	FeO	CoO	NiO	ZnO	Total
#101	ol	21	0.00	39.1	0.01	38.9	n.a.	0.00	0.04	0.01	n.a.	0.02	0.43	22.0	n.a.	n.a.	n.a.	100.5
			(.00)	(.3)	(.02)	(.3)		(.00)	(.03)	(.01)		(.03)	(.01)	(.3)				
	low-Ca px	29	0.01	29.0	0.15	55.9	n.a.	0.00	0.74	0.17	n.a.	0.08	0.43	13.4	n.a.	n.a.	n.a.	99.9
			(.01)	(.3)	(.06)	(.3)		(.00)	(.13)	(.05)		(.04)	(.01)	(.5)				
	fld	37	9.67	0.04	21.0	66.0	n.a.	0.94	2.05	0.02	n.a.	0.03	0.02	0.52	n.a.	n.a.	n.a.	100.3
			(.44)	(.05)	(.4)	(.7)		(.31)	(.17)	(.02)		(.04)	(.02)	(.19)				
	chr	13	0.01	2.95	5.73	0.11	0.01	0.00	0.03	3.13	0.63	54.7	0.69	30.1	0.03	0.03	0.26	98.4
			(.01)	(.27)	(.08)	(.10)	(.02)	(.00)	(.03)	(.11)	(.04)	(.6)	(.04)	(.5)	(.01)	(.03)	(.05)	
	phos	3	2.59	3.47	0.00	0.01	46.2	0.04	47.1	0.00	n.a.	0.00	0.03	0.47	n.a.	n.a.	n.a.	99.6
			(.06)	(.04)	(.00)	(.02)	(.3)	(.01)	(.1)	(.00)		(.00)	(.01)	(.05)				
#201	ol	15	0.00	39.0	0.01	38.8	n.a.	0.00	0.02	0.01	n.a.	0.09	0.42	21.9	n.a.	n.a.	n.a.	100.3
			(.00)	(.2)	(.03)	(.2)		(.00)	(.01)	(.02)		(.33)	(.01)	(.2)				
	low-Ca px	23	0.02	28.9	0.15	55.9	n.a.	0.00	0.85	0.15	n.a.	0.08	0.43	13.1	n.a.	n.a.	n.a.	99.6
			(.01)	(.2)	(.04)	(.3)		(.00)	(.10)	(.04)		(.03)	(.02)	(.3)				
	opx	2	0.03	27.5	1.73	54.4	n.a.	0.00	1.63	0.11	n.a.	1.18	0.38	12.8	n.a.	n.a.	n.a.	99.8
			(.05)	(.3)	(.36)	(.2)		(.00)	(.18)	(.03)		(.01)	(.05)	(.2)				
	fld	13	9.77	0.05	20.9	66.3	n.a.	0.60	1.96	0.02	n.a.	0.03	0.02	0.28	n.a.	n.a.	0.05	100.0
			(.23)	(.06)	(.4)	(.6)		(.11)	(.20)	(.02)		(.03)	(.03)	(.12)			(.05)	
	chr	11	0.02	2.36	4.05	0.12	0.01	0.00	0.02	2.95	0.78	55.6	0.68	30.5	0.03	0.03	0.46	97.6
			(.02)	(.37)	(.55)	(.11)	(.01)	(.00)	(.02)	(.45)	(.08)	(.7)	(.07)	(.6)	(.02)	(.03)	(.05)	
#202	ol	30	0.01	40.0	0.01	38.8	n.a.	0.00	0.02	0.03	n.a.	0.01	0.42	20.9	n.a.	n.a.	n.a.	100.1
			(.01)	(.3)	(.01)	(.2)		(.00)	(.01)	(.03)		(.01)	(.01)	(.4)				
	low-Ca px	22	0.01	30.4	0.24	56.3	n.a.	0.00	0.42	0.05	n.a.	0.22	0.35	11.8	n.a.	n.a.	n.a.	99.8
			(.01)	(1.4)	(.19)	(.5)		(.00)	(.38)	(.04)		(.13)	(.10)	(1.8)				
	fld	2	5.11	0.08	28.8	55.0	n.a.	0.05	10.8	0.03	n.a.	0.03	0.05	0.25	n.a.	n.a.	0.00	100.1
			(.65)	(.08)	(.4)	(1.3)		(.01)	(.5)	(.01)		(.02)	(.03)	(.01)			(.00)	
	chr	9	0.03	1.83	4.32	0.23	0.02	0.00	0.02	1.57	0.70	57.7	0.72	30.1	0.04	0.03	0.49	97.9
			(.02)	(.11)	(.24)	(.17)	(.02)	(.00)	(.03)	(.09)	(.03)	(.7)	(.05)	(.4)	(.01)	(.03)	(.05)	

Numbers in parentheses represent standard deviations. n = number of analyses. ol = olivine, low-Ca px = low-Ca pyroxene, opx = orthopyroxene, pig = pigeonite, aug = augite, fld = feldspar, chr = chromite, sp = spinel, phos = Ca-phosphate, gl = glass. n.a. = not analyzed.

Table 1. Continued.

clast	phase	n	Na2O	MgO	Al2O3	SiO2	P2O5	K2O	CaO	TiO2	V2O3	Cr2O3	MnO	FeO	CoO	NiO	ZnO	Total
matrix	ol	44	0.00	40.0	0.01	39.0	n.a.	0.00	0.04	0.02	n.a.	0.02	0.45	21.7	n.a.	n.a.	n.a.	101.2
			(.01)	(.76)	(.02)	(.3)		(.00)	(.02)	(.03)		(.05)	(.02)	(.9)				
	low-Ca px	56	0.02	29.6	0.19	56.2	n.a.	0.00	0.64	0.15	n.a.	0.17	0.46	13.2	n.a.	n.a.	n.a.	100.6
			(.02)	(1.1)	(.14)	(.6)		(.00)	(.19)	(.10)		(.22)	(.04)	(1.6)				
	opx	3	0.06	28.5	1.03	55.3	n.a.	0.00	1.37	0.15	n.a.	0.53	0.46	12.3	n.a.	n.a.	n.a.	99.7
			(.04)	(.3)	(.98)	(1.3)		(.00)	(.41)	(.08)		(.38)	(.01)	(.2)				
	aug	2	0.25	22.8	0.29	55.0	n.a.	0.00	11.8	0.29	n.a.	0.37	0.34	8.91	n.a.	n.a.	n.a.	100.0
			(.13)	(3.1)	(.03)	(.7)		(.00)	(4.2)	(.06)		(.11)	(.04)	(1.98)				
	fld	43	9.50	0.07	21.2	65.4	n.a.	0.95	2.34	0.04	n.a.	0.02	0.02	0.52	n.a.	n.a.	0.01	100.0
			(1.31)	(.09)	(1.9)	(3.1)		(.30)	(2.28)	(.04)		(.05)	(.02)	(.25)			(.03)	
	chr	43	0.02	2.72	5.38	0.13	0.02	0.00	0.03	2.63	0.66	55.5	0.71	30.0	0.03	0.03	0.33	98.1
			(.02)	(.55)	(.95)	(.13)	(.02)	(.00)	(.04)	(.45)	(.06)	(1.5)	(.08)	(.9)	(.02)	(.04)	(.17)	
	sp	1	0.00	11.5	45.9	0.08	0.00	0.00	0.00	0.11	0.13	19.7	0.27	20.6	0.00	0.00	0.83	99.0
#154	ol	4	0.00	56.7	0.31	43.1	n.a.	0.00	0.53	0.08	n.a.	0.06	0.01	0.45	n.a.	n.a.	n.a.	101.2
			(.00)	(.1)	(.11)	(.4)		(.00)	(.06)	(.02)		(.03)	(.01)	(.11)				
	gl	3	7.80	0.37	29.5	57.8	n.a.	0.99	0.58	1.28	n.a.	0.23	0.07	1.80	n.a.	n.a.	n.a.	100.4
			(.46)	(.16)	(1.8)	(3.0)		(.44)	(.31)	(.14)		(.03)	(.02)	(.34)				
#209	ol	5	0.01	42.4	0.14	39.8	n.a.	0.00	0.17	0.02	n.a.	0.28	0.21	17.6	n.a.	n.a.	n.a.	100.6
			(.01)	(10.6)	(.14)	(2.4)		(.00)	(.07)	(.02)		(.27)	(.15)	(12.6)				
	opx	1	0.12	32.0	1.50	56.5	n.a.	0.00	1.24	0.18	n.a.	0.99	0.34	7.48	n.a.	n.a.	n.a.	100.3
	pig	1	0.08	30.8	2.21	56.2	n.a.	0.00	3.67	0.31	n.a.	1.51	0.49	4.56	n.a.	n.a.	n.a.	99.8
	fld	2	3.56	0.42	30.0	51.2	n.a.	0.09	13.2	0.08	n.a.	0.08	0.03	0.65	n.a.	n.a.	0.07	99.4
			(.18)	(.24)	(.2)	(.4)		(.04)	(.6)	(.04)		(.01)	(.00)	(.22)			(.10)	
	gl	3	8.06	2.20	24.5	59.4	n.a.	0.33	0.54	1.02	n.a.	0.85	0.03	2.35	n.a.	n.a.	0.03	99.3
			(.39)	(.51)	(.2)	(.7)		(.03)	(.37)	(.02)		(.19)	(.06)	(.18)			(.02)	
#134	ol	8	0.01	40.0	0.04	39.4	n.a.	0.00	0.05	0.02	n.a.	0.03	0.02	21.1	n.a.	n.a.	n.a.	101.1
			(.01)	(.3)	(.04)	(.3)		(.00)	(.02)	(.01)		(.02)	(.45)	(.3)				
	low-Ca px	3	0.01	34.5	0.29	58.1	n.a.	0.00	0.38	0.07	n.a.	0.34	0.24	7.08	n.a.	n.a.	n.a.	101.0
			(.02)	(3.9)	(.07)	(2.5)		(.00)	(.04)	(.06)		(.14)	(.14)	(5.64)				
	pig	1	0.12	29.55	1.10	56.1	n.a.	0.00	3.26	0.21	n.a.	0.70	0.40	8.96	n.a.	n.a.	n.a.	100.4
	aug	4	0.33	19.9	4.47	52.8	n.a.	0.00	17.8	0.97	n.a.	1.32	0.40	1.73	n.a.	n.a.	n.a.	99.7
			(.18)	(2.7)	(1.33)	(1.6)		(.00)	(1.8)	(.22)		(.11)	(.06)	(.28)				

matrix are shown in Table 1. In most clasts, the 100 Fe/(Fe+Mg) atomic ratios of olivine and low-Ca pyroxene are within the range of those in equilibrated L-group chondrites (*i.e.*, Fa_{22-25} and Fs_{19-22}). Thus they are fragments of equilibrated L-group chondrtite. Some clasts contain olivine and low-Ca pyroxene with wider ranges of Fe/(Fe+Mg) ratios, suggesting that they are fragments of less equilibrated chondrites. The "equilibrated clasts" are defined as clasts with both equilibrated olivine and low-Ca pyroxene in which the Fe/(Fe+Mg) ratios are characteristic of equilibrated L-group chondrites. The "unequilibrated clasts" are defined as clasts with unequilibrated olivine and/or low-Ca pyroxene (Fig. 1).

3.2. Clasts

Three chondritic clasts, #101, #201 and #202 (Fig. 2) are large enough to define their petrologic type (Van Schmus and Wood, 1967) and shock features. Clasts #101 and # 201 are petrographically indistinguishable from average L5 and L6 chondrites, respectively. They contain olivine and low-Ca pyroxene with compositions within the ranges of equilibrated L-group chondrites (Fig. 3). Chondrules in clasts #101 and #201 exhibit recrystallized boundaries and do not contain any glass. Chondrules in clast #101 are readily delineated, whereas those in clast #201 are fragmented and poorly defined. The presence of undulatory extinction and planar fractures in olivine grains indicates that the shock stage of clasts #101 and #201 is S3. As shown in Figs. 2 and 3, clast #202 is a fragment of an L4 chondrite, consisting of homogeneous olivine with heterogeneous low-Ca pyroxene ($Fs_{9.7-21}$). Chondrule-matrix boundaries are sharply defined. Mesostases of chondrules are devitrified and mainly of feldspar composition ($An_{51-56}Or_{0.3}$). Olivine shows undulatory extinction, planar fractures and mosaicism, indicating that the shock stage of clast #202 is S4.

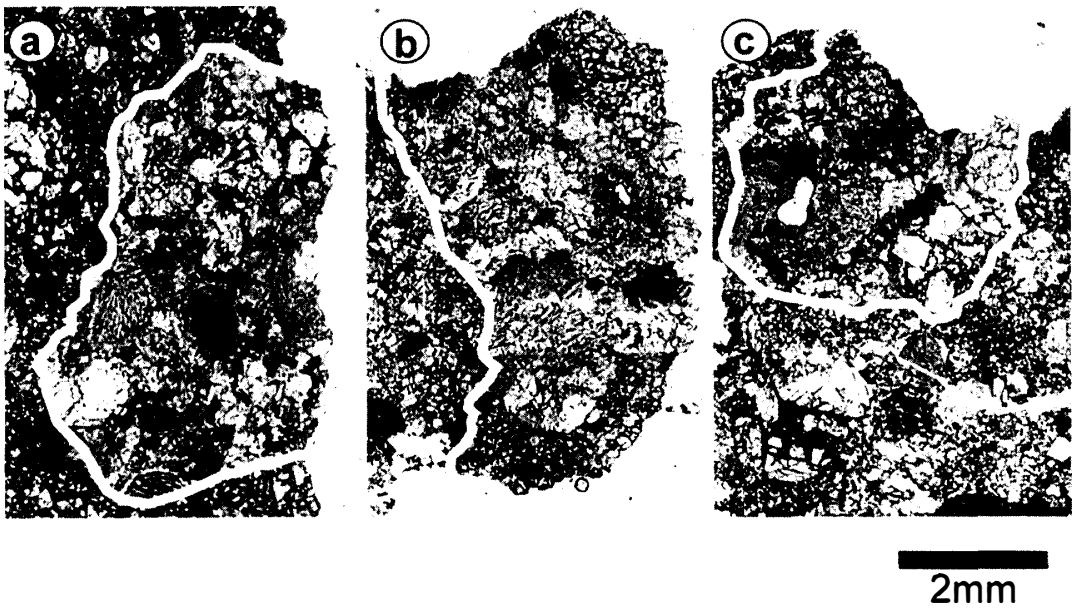

Fig. 2. Photomicrographs of three large clasts in ALH-77252 (plane polarized light). a) #101, type-5 chondritic clast. b) #201, type-6 chondritic clast. c) #202, type-4 chondritic clast.

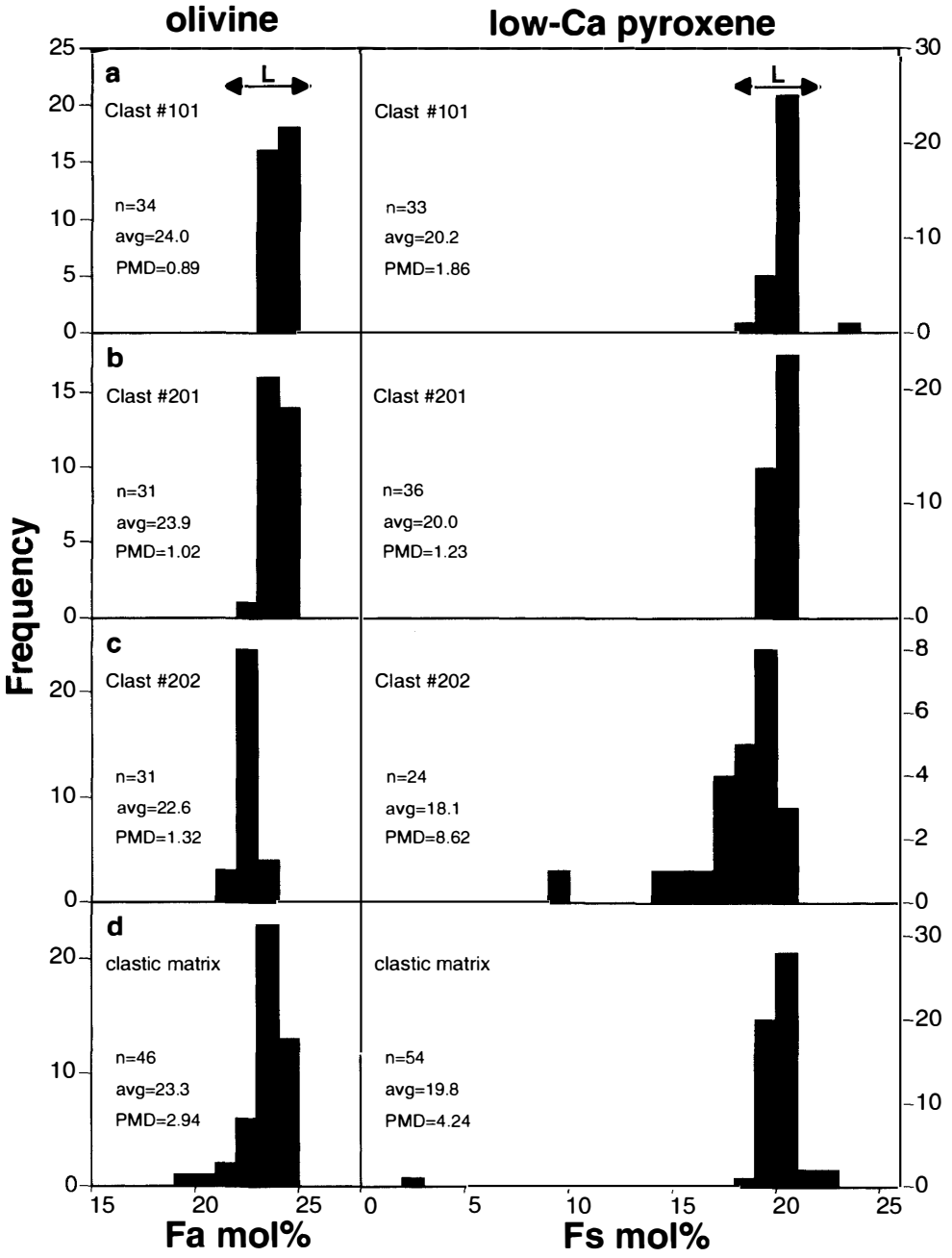

Fig. 3. Histograms of Fa and Fs contents in olivine and low-Ca pyroxene in the clasts and clastic matrix. (a) #101, (b) #201, (c) #202 and (d) clastic matrix. Analytical points were selected by randomly. Ranges of average L-group chondrite are shown by arrows. n=number of analyses, avg=average, PMD=percent mean deviation.

Unequilibrated clasts are occasionally surrounded by fine-grained iron-rich olivine aggregates, which are similar to fine-grained matrices/rims found in some UOCs (Ashworth, 1977; Huss *et al.*, 1981). Olivine and low-Ca pyroxene in unequilibrated clasts exhibit a wide range of Fe/(Fe+Mg) ratios ($Fa_{0.4\text{-}49}$ and $Fs_{0.8\text{-}37}$) and most grains are less Fe-rich than those in equilibrated L-group chondrites. Normal Fe-Mg zoning is

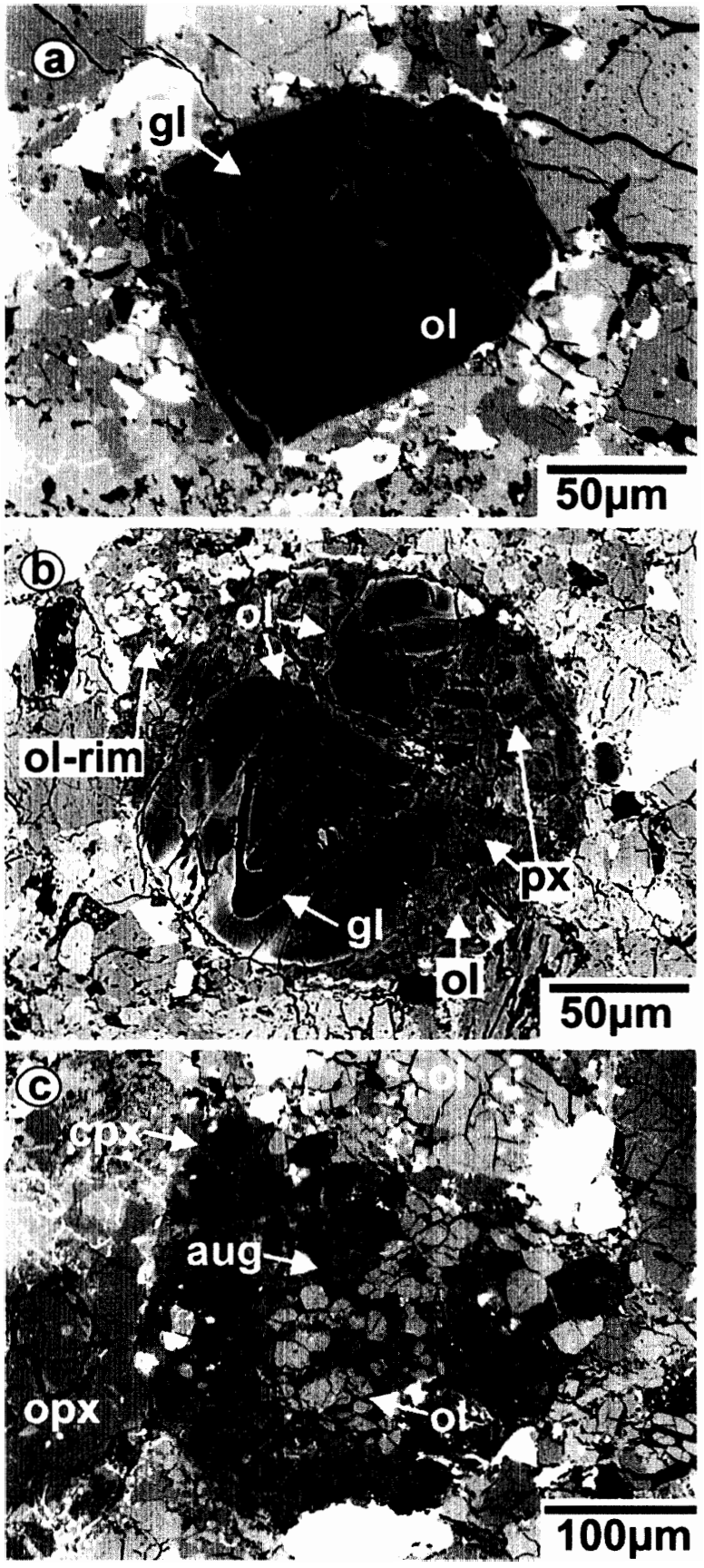

Fig. 4. Backscattered electron images of unequilibrated clasts in ALH-77252. (a) #154, fragment of BO chondrule with slightly zoned olivine (ol) and glass (gl). (b) #209, POP-BO compound chondrule with unequilibrated olivine and low-Ca pyroxene surrounded by discrete Fa-rich olivine rim (ol-rim). (c) #134, fragment of POP chondrule with equilibrated olivine, unequilibrated low-Ca pyroxene and augite (aug).

preserved in most unequilibrated olivine and low-Ca pyroxene grains. In some cases, unequilibrated chondrules contain mesostasis glasses.

Barred olivine (BO) chondrule fragment #154 is one of the least metamorphosed clasts we examined. It is composed of clear glass and iron-poor ($Fa_{0.4}$ in the core) olivine (Fig. 4a). Olivine shows Fe-Mg zoning of less than 2 μm-width from the contact with clastic matrix. A compound porphyritic olivine-pyroxene (POP) chondrule #209 contains a BO chondrule (Fig. 4b). Iron-rich olivine rim is observed in the outer parts of the POP chondrule. The inner BO chondrule has glassy mesostases and the outer POP chondrule contains calcic feldspar (An_{67}). Both olivine and low-Ca pyroxene in #209 show normal Fe-Mg zoning. In a fragment of a POP chondrule #134, olivine compositions are homogeneous (Fa_{22-23}) as in equilibrated L-group chondrites, while low-Ca pyroxenes are heterogeneous ($Fs_{4.7-20}$) (Fig. 4c). Augite ($Wo_{38}Fs_{2.9}$) and olivine (Fa_{22-23}) grains are poikilitically enclosed by several twinned grains of low-Ca clinopyroxene. low-Ca clinopyroxene is rimmed by pigeonite.

3.3. Clastic matrix

The clastic matrix consists mainly of olivine, pyroxene, feldspar, iron-sulfides and Fe-

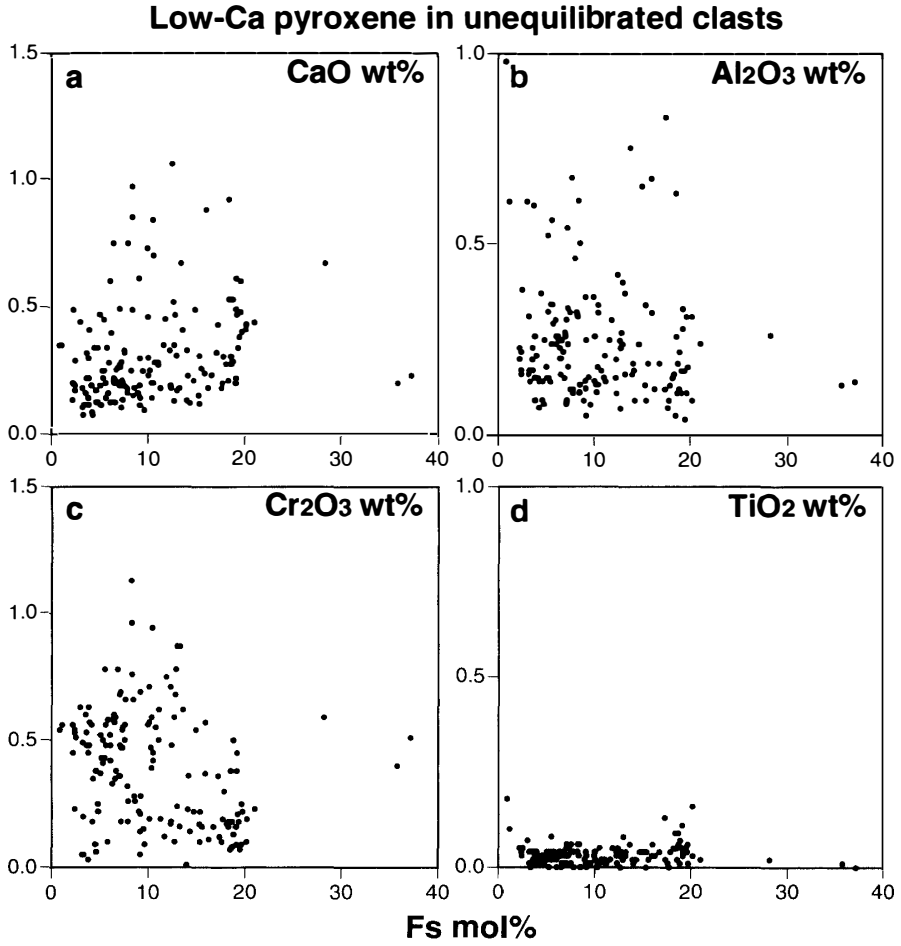

Fig. 5. Plots of minor element contents (a, CaO; b, Al_2O_3; c, Cr_2O_3; d, TiO_2) against the Fs composition of low-Ca pyroxene in unequilibrated clasts.

Ni metal with minor phases such as chromite, Ca-phosphate and Mg-rich spinel. The clastic matrix is dark in color under the transmitted light because of the presence of fine-grained opaque minerals. Unequilibrated olivine and low-Ca pyroxene are observed in the clastic matrix (Fig. 3). During the course of random analyses of clastic matrix, we found slightly Mg-enriched olivine (Fa_{20}) and Mg-rich low-Ca pyroxene ($Fs_{3.0}$).

3.4. Mineral chemistry

low-Ca pyroxene: low-Ca pyroxene in equilibrated clasts is dominantly orthopyroxene, whereas unequilibrated clasts both orthopyroxene and clinopyroxene occur. Twinned clinopyroxene occasionally occurs in equilibrated clasts and is frequently observed in unequilibrated ones. Some low-Ca pyroxenes are surrounded by pigeonite or augite rims up to Wo_{46}. Compared with low-Ca pyroxene, pigeonite and augite are rich in Al_2O_3, Cr_2O_3 and TiO_2.

In Figs. 5–7, CaO, Al_2O_3, Cr_2O_3 and TiO_2 contents in low-Ca pyroxene in unequilibrated clasts, equilibrated clasts and clastic matrix are plotted against Fs contents. In general, CaO and TiO_2 contents in low-Ca pyroxene in equilibrated clasts are higher than in low-Ca pyroxene in unequilibrated clasts (Table 2). On the other hand, Al_2O_3 and

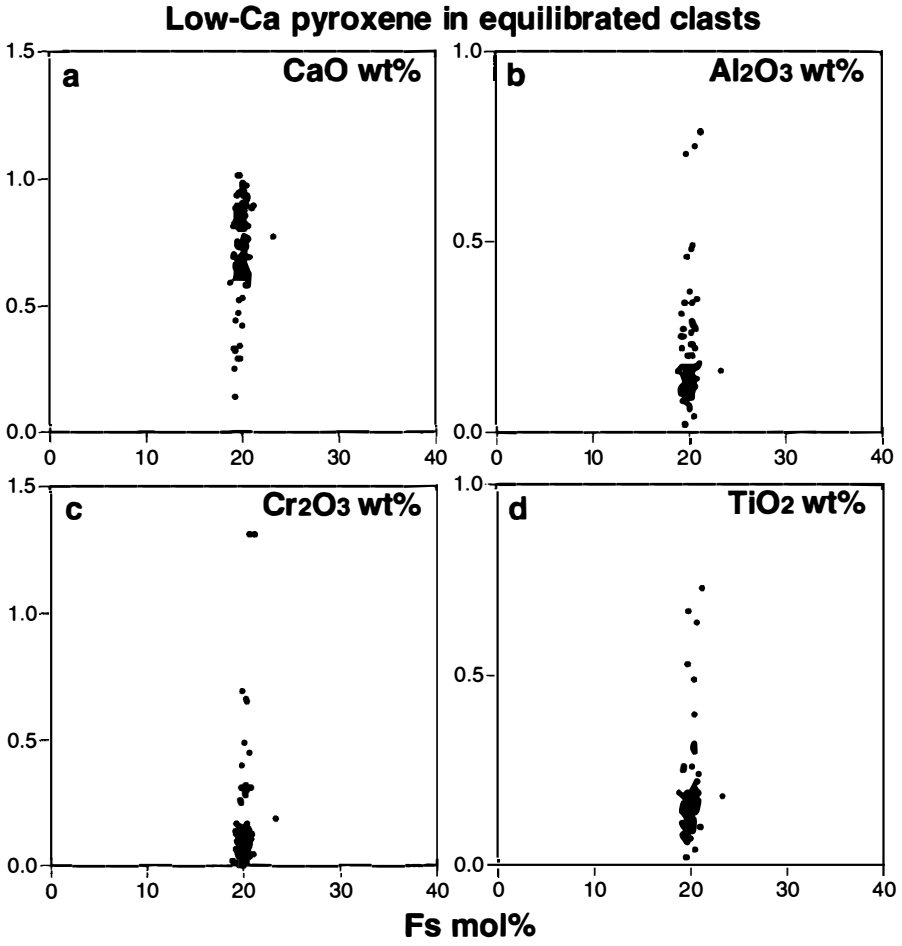

Fig. 6. Plots of minor element contents (a, CaO; b, Al_2O_3; c, Cr_2O_3; d, TiO_2) against the Fs composition of low-Ca pyroxene in equilibrated clasts.

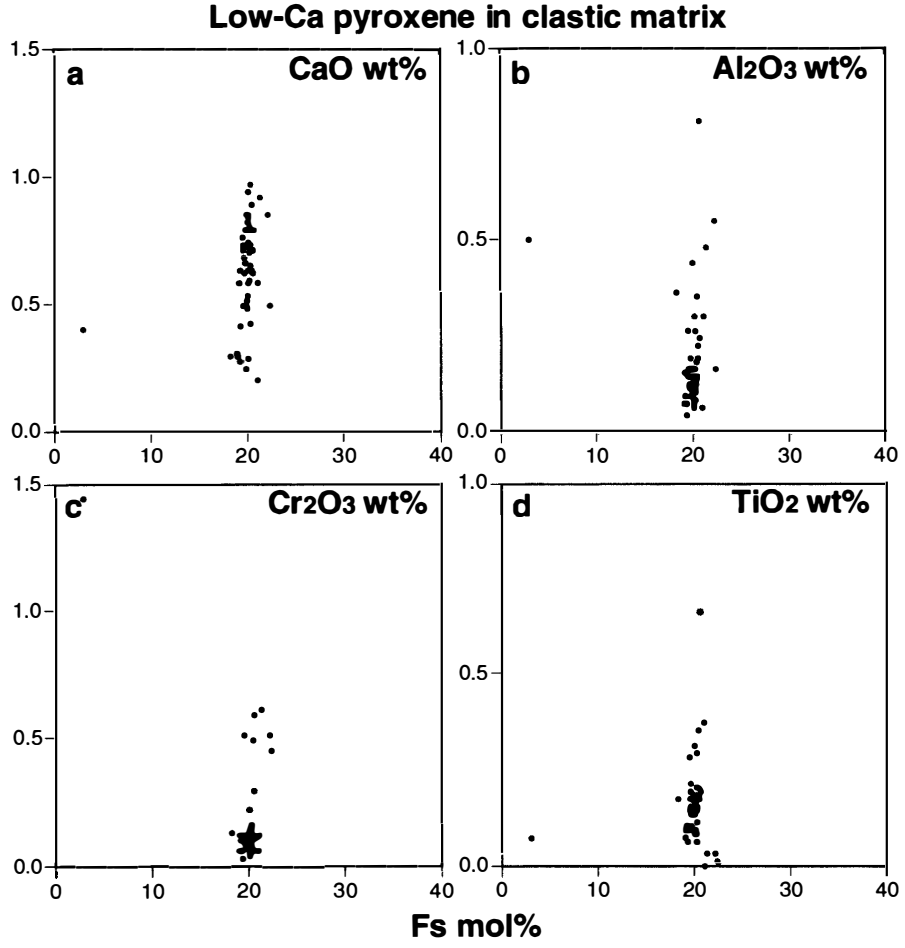

Fig. 7. Plots of minor element contents (a, CaO; b, Al_2O_3; c, Cr_2O_3; d, TiO_2) against the Fs composition of low-Ca pyroxene in the clastic matrix.

Talbe 2. Average concentrations (wt%) of minor elements.

	n	CaO	Al2O3	TiO2	Cr2O3
unequilibrated clast	156	0.31 (0.20)	0.24 (0.16)	0.03 (0.03)	0.39 (0.23)
equilibrated clast	133	0.73 (0.16)	0.18 (0.12)	0.17 (0.10)	0.13 (0.19)
clastic matrix	56	0.64 (0.19)	0.19 (0.14)	0.15 (0.10)	0.17 (0.22)

Numbers in parentheses represent standard deviations. n = number of analyses.

Cr_2O_3 contents in low-Ca pyroxene in equilibrated clasts are similar to or somewhat lower than those in unequilibrated clasts (Figs. 5 and 6). The trends of minor element contents in low-Ca pyroxene are similar to those observed in Weston, an H3-7 regolith breccia (Noonan and Nelen, 1976). The minor element signatures of most low-Ca pyroxenes in the clastic matrix are indistinguishable from those in equilibrated clasts (Fig. 7). In the titanium *versus* aluminum and titanium *versus* chromium diagrams, two distinct clusters are observed (Fig. 8). Low-Ca pyroxene in unequilibrated clasts has a low Ti/Al ratio (~0.07), while Ti/Al ratio of most low-Ca pyroxene in equilibrated clasts are high (~0.5). In both equilibrated and unequilibrated clasts, Ti/Cr ratios of low-Ca pyroxene are

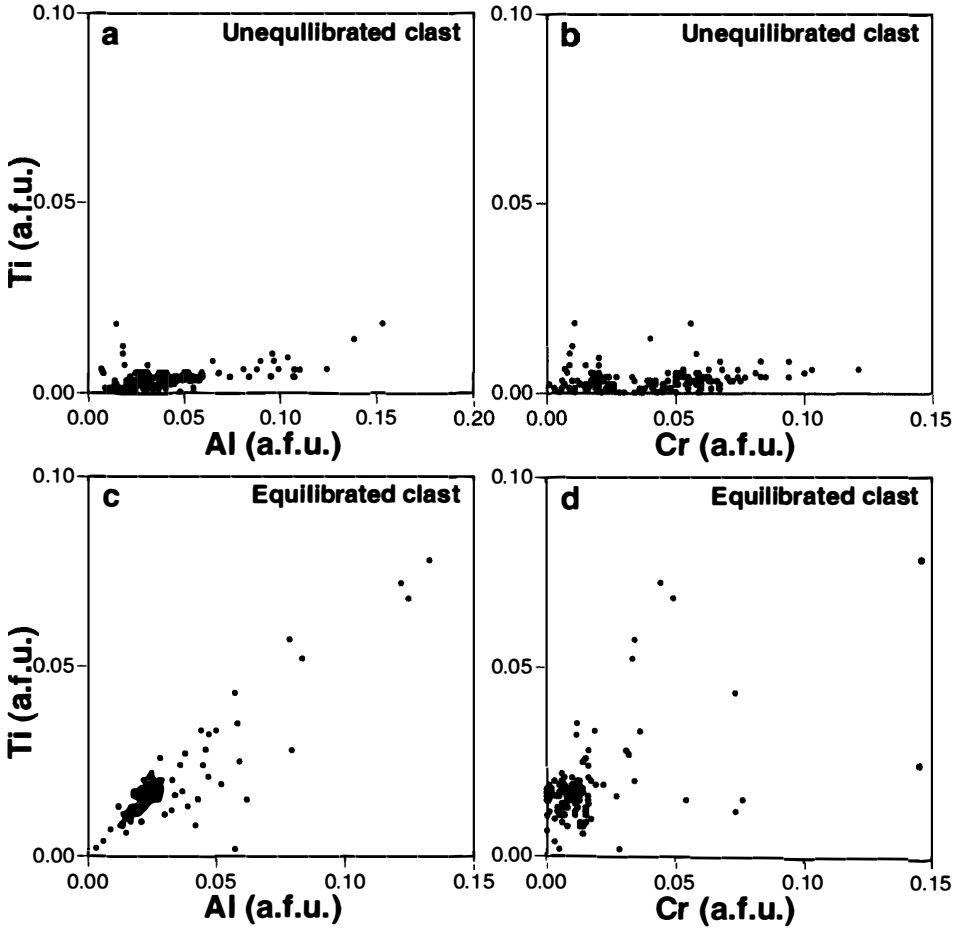

Fig. 8. Interrelation of atomic number ratios between titanium versus aluminum and titanium versus chromium of unequilibrated clasts (a, b) and equilibrated clasts (c, d). Both diagrams show two distinct clustering of equilibrated and unequilibrated low-Ca pyroxenes. a.f.u.=atomic formula unit per 24 oxygen.

variable.

Olivine: In Fig. 9, CaO, Al_2O_3, Cr_2O_3 and TiO_2 contents in olivine in unequilibrated clasts, equilibrated clasts and clastic matrix are plotted against Fa contents. Olivine is generally poor in Al_2O_3 and TiO_2, especially in equilibrated clasts. Some olivines with iron-poor compositions in unequilibrated clasts are rich in CaO. Olivine in unequilibrated clasts is rich in Cr_2O_3 in comparison with that in equilibrated clasts.

Feldspar: Compositions of feldspar in equilibrated clasts are generally within a narrow range of $An_{10\text{-}15}Or_{0\text{-}10}$ (Fig. 10), which is consistent with those in equilibrated L-group chondrites (Brearley and Jones, 1998). Some unequilibrated clasts contain more calcic feldspars (up to An_{67}) similar to those in unequilibrated L-group chondrites (Brearley and Jones, 1998). Among the clasts we examined (#101, #201 and #202), there is no relationship between petrologic type and feldspar composition.

Chromite: Compositions of chromite in equilibrated clasts are less variable and tend to have higher Al_2O_3 than those in clastic matrix (Fig. 11). Chromites in the unequilibrated clast #202 are poorer in Al_2O_3 and similar to some chromites in the clastic matrix.

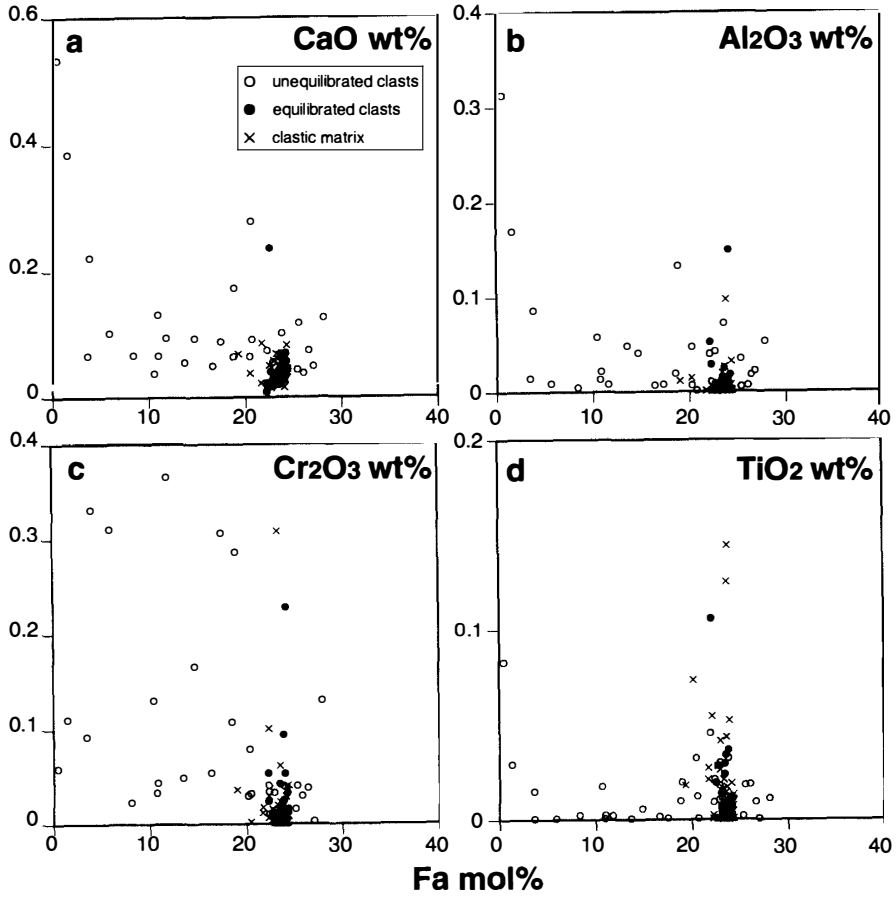

Fig. 9. Plots of minor element contents (a, CaO; b, Al_2O_3; c, Cr_2O_3; d, TiO_2) against the Fa composition of olivine in the unequilibrated clasts, equilibrated clasts and clastic matrix. Compositions of olivine in equilibrated clasts are poorer in these minor elements in comparison with unequilibrated clasts.

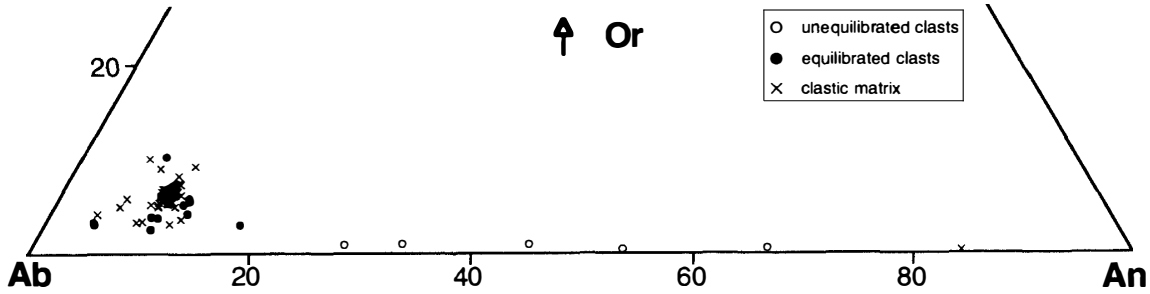

Fig. 10. Feldspar compositions in unequilibrated clasts, equilibrated clasts and clastic matrix. Distribution patterns of equilibrated clasts and unequilibrated clasts are consistent with typical composition of feldspar in L3 and those in L4-6 chondrites, respectively (Brearley and Jones, 1998).

4. Discussion

4.1. Major element compositions of olivine and pyroxene

ALH-77252 is composed of clasts of various metamorphic grades from type-4 to -6.

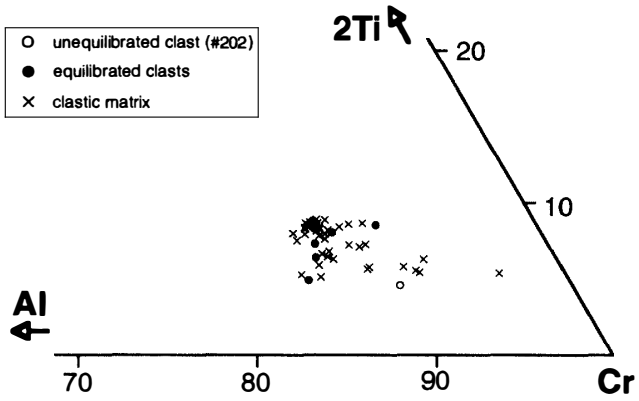

Fig. 11. Chromite compositions in the unequilibrated clast (#202), equilibrated clasts and clastic matrix. Some chromites in the clastic matrix are poorer in Al_2O_3 than those in the equilibrated clasts. The similarity in composition indicates that the matrix chromites are fragments of unequilibrated clasts.

We also found type-3 like clasts which consist of heterogeneous olivine and/or glass. They are consistent with previous observations (Scott, 1984). Compositional ranges of minor elements in olivine, pyroxene and feldspar seem to simply reflect an admixture of EOC fragments with minor UOC fragments. No foreign clast with different characteristics from L-group chondritic materials was observed in this study.

The effect of thermal metamorphism in OC is the chemical homogenization of constituent olivine and low-Ca pyroxene. During thermal metamorphism, Fe-Mg in olivine and low-Ca pyroxene are homogenized progressively but not simultaneously. ALH-77252 is dominated by fragments of EOCs with equilibrated olivine and low-Ca pyroxene, which may have suffered prolonged/intense thermal metamorphism. Because the diffusion rate of Fe^{2+} in olivine is much higher than in low-Ca pyroxene (Ganguly and Tazzoli, 1993), Fe/(Fe+Mg) homogenization in olivine progresses more rapidly than that in coexisting low-Ca pyroxene (Dodd *et al.*, 1967; Scott, 1984; Tsuchiyama *et al.*, 1988; McCoy *et al.*, 1991). The presence of equilibrated olivine coexisting with unequilibrated low-Ca pyroxene in some unequilibrated clasts indicates that these clasts suffered thermal metamorphism, but the degree of thermal metamorphism was insufficient to homogenize low-Ca pyroxene. Thus, the effects of thermal metamorphism vary among unequilibrated clasts and on to equilibrated clasts in ALH-77252, which is consistent with the complete metamorphic sequence of petrologic type-3 to -6. We found (1) olivine with a wide range of Fa contents, (2) unequilibrated clasts containing clear glasses and (3) Fe-Mg zoning of olivine at the margin of the least metamorphosed clast #154. These features indicate that ALH-77252 did not suffer significant thermal metamorphism after they were agglomerated into the present condition. Thus the observed variations of metamorphic grades in the clasts reflect primary features caused by thermal metamorphism of individual clasts prior to brecciation.

4.2. Minor element compositions of low-Ca pyroxene

As shown in Fig. 8, interrelationships of aluminum, titanium and chromium are different between equilibrated and unequilibrated low-Ca pyroxenes. If the minor element compositions of low-Ca pyroxene changed gradually during thermal

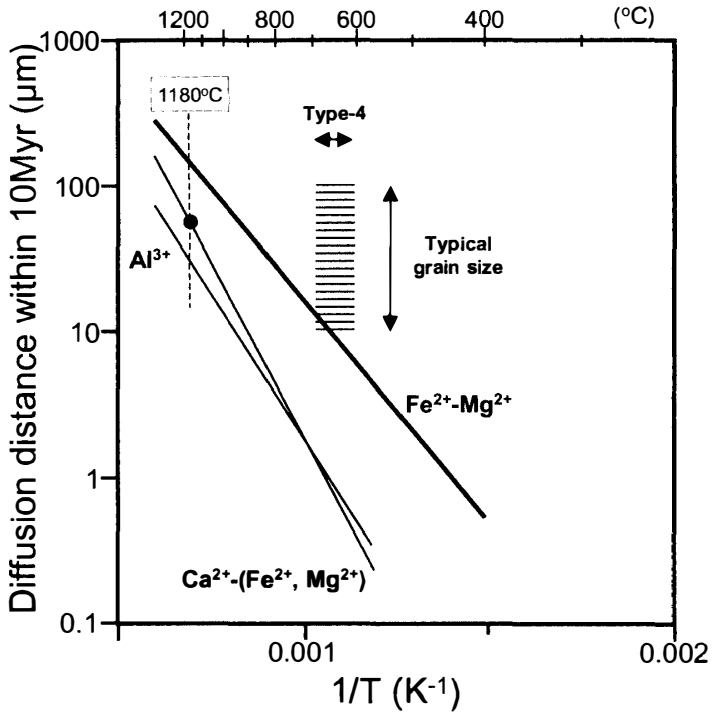

Fig. 12. The diffusion distance of cations in pyroxene within 10 Myr. The diffusion coefficients of Fe^{2+}-Mg^{2+} and Ca^{2+}-(Fe^{2+}, Mg^{2+}) are given by Ganguly and Tazzoli (1992) and Brady and McCallister (1983), respectively. The diffusion coefficient of Al^{3+} is calculated from the diffusion coefficient at 1180°C in clinopyroxene and activation energy in omphacite (Sautter et al., 1988; Carpenter 1981). Diffusion distance is given as $\sqrt{Dt}$, where D is diffusion coefficient and t is time. Metamorphic temperatures of type-4 chondrite are from Dodd (1981).

metamorphism, the observed distribution of minor elements is hard to explain. The simplest explanation is that this compositional gap could be resulted from the unrepresentative sampling of the source regolith. However, similar trends are clearly observed in the published database of low-Ca pyroxene in LL-group chondrites (Jones and Scott, 1989; Jones, 1990, 1994; Heyse, 1978; McSween and Patchen, 1989; McCoy *et al.*, 1991). Thus we suggest that the observed differences between equilibrated and unequilibrated low-Ca pyroxenes in ALH-77252 clasts are not special but may represent chemical characteristics of OCs.

There are two possibilities for the large differences in minor element compositions in low-Ca pyroxenes: (1) minor elements were redistributed during thermal metamorphism, or (2) low-Ca pyroxene preserved its initial signature of minor elements to some extent. In the former case, both equilibrated and unequilibrated low-Ca pyroxenes were derived from similar initial compositions, *i.e.*, poor in calcium and titanium, and rich in aluminum and chromium. During thermal metamorphism, calcium and titanium were incorporated into low-Ca pyroxene whereas chromium and aluminum were not. Diffusion of calcium, titanium and aluminum should have occurred at higher temperature than Fe-Mg homogenization. In the latter case, the observed differences between equilibrated and unequilibrated low-Ca pyroxene were inherited mainly from different conditions of low-Ca

pyroxene crystallization. Because most of the low-Ca pyroxenes we examined would be derived from chondrules and their fragments, minor element compositions of low-Ca pyroxene could reflect primarily the bulk chemistry of chondrule melts along with redox conditions and cooling histories during chondrule formation.

Metamorphic redistribution of minor elements in low-Ca pyroxene would have been caused by subsolidus diffusion of cations. Mittlefehldt and Lindstrom (2001) found a difference in Al/Ti ratios between an L7 chondrite and a clast-poor impact-melt breccia, and attributed the difference to the result of crystallization zoning and diffusional equilibration. Unfortunately, diffusion coefficients in low-Ca pyroxene of minor elements, such as calcium, aluminum, titanium, and chromium have not yet been precisely determined. The temperature dependence of the diffusion coefficient D is described by an Arrhenius equation $D = D_0 \exp(-Q/RT)$, where T is temperature, D_0 is a pre-exponential factor and R is the gas constant. Calcium in clinopyroxene ($Na_{0.1}Ca_{0.53}Mg_{1.1}Fe_{0.17}Al_{0.1}Si_2O_6$) has a pre-exponential factor $D_0 = 10^{-6.432}$ m^2/s with an activation energy of $Q = 360.87$ kJ/mol (Brady, 1995). If calcium in low-Ca pyroxene has a similar diffusivity, a metamorphic temperature of 770–900°C is required to achieve the significant mobility (10–100 μm/10 Myr) of calcium in the pyroxene structure. Aluminum and titanium are not so diffusive in the pyroxene structure (Huebner, 1980). Aluminum diffusivity of $D = 3.2 \times 10^{-21}$ m^2/s at 1180°C in diopside (Sautter *et al.*, 1988) and the activation energy of Q=300 kJ/mol in omphacites (Carpenter, 1981) were obtained experimentally. Figure 12 illustrates the relations between the inferred diffusion distance of aluminum, calcium, iron and magnesium wihin 10 Myr, and ambient temperature. Although the uncertainties in evaluation of diffusivities for these elements could be large, aluminum and calcium seem to diffuse very slowly in the pyroxene structure. When these evaluations are applied to low-Ca pyroxene, a metamorphic temperature of 790–950°C is required for significant mobilization of aluminum. Because Ti^{4+} and Ti^{3+} in the octahedral site of pyroxene have larger ionic radii than Al^{3+} in the same site, titanium is also regarded as an immobile element. The immobility of minor elements in low-Ca pyroxene would provide considerable restriction for the thermal history of OCs.

4.3. Implications for thermal history of L chondrite parent body

The clasts with different metamorphic grades in ALH-77252 could not have coexisted during thermal metamorphism. Thus they should have originated from separate locations on the parent body. In order to explain the coexistence of clasts with different metamorphic degrees in some chondritic breccia and the lack of any correlation between metallographic cooling rates and petrologic types of OCs, break-up and reassembly of chondrite parent bodies were proposed (Keil, 1982; Scott and Rajan, 1981; Taylor *et al.*, 1987). Break-up of a parent body could have been induced by disruptive collision of planetesimals of comparable sizes. Subsequent reassembly would be driven by gravitation within a short time scale, resulting in a rubble-pile parent body (Grimm, 1985). The surface of rubble-pile body would have contained clasts of various metamorphic grades from extensive region of the parent body. ALH-77252 would have been lithified on the surface regolith of the rubble-pile body.

Correlation between petrologic type and shock degree, and some lines of petrologic evidence for localized thermal metamorphism induced by impact support the idea that

impact could be heat source of thermal metamorphism of OCs (*e.g.*, Rubin, 1995). Thermal metamorphism with initially higher temperature induced by impact seems to be somewhat reasonable to explain the rapid diffusion of minor elements in low-Ca pyroxene. However, there is considerable difficulty in the parent body sizes, because both single disruptive collision and cumulative multiple impacts can cause only a limited scale of thermal effect on the parent body of less than a few hundreds of kilometers (Keil *et al.*, 1997). Although impacts could have played an important role for the thermal history of OCs with structural modification of parent body by disruptive collision, impact heating itself seems to have been ineffective for the global heating of parent body of OCs.

The most plausible heat source for thermal metamorphism of chondrite parent bodies is short-lived radioactive nuclides ^{26}Al (*e.g.*, Lee *et al.*, 1976; McSween *et al.*, 1988). If we suppose such internal heat source for the thermal metamorphism, the parent body would have primarily an onion-shell structure in which rocks were highly metamorphosed at the inner core and least affected at the outer rim (*e.g.*, Miyamoto *et al.*, 1981; Bennet and McSween, 1996). Thermodynamic model calculation showed that thermal metamorphism induced by the heat from ^{26}Al decay would have continued for 10 Myr for type-3 to -5 OCs and for 100 Myr for type-6 OCs (Miyamoto *et al.*, 1981; Bennet and McSween, 1996). If this was the case, type-4 and type-5 OCs have suffered from thermal metamorphism for ~10 Myr with temperature of 600–700°C and 700–750°C (Dodd, 1981), respectively. However, the metamorphic temperature of more than ~800°C is required to obtain enough mobility of titanium and aluminum in low-Ca pyroxene with the size of a few tens of micrometers (Fig. 12). It appears that drastic changes in Ti/Al ratios of low-Ca pyroxene was hardly attained during thermal metamorphism. Thus we suggest that the minor element signatures observed in equilibrated and unequilibrated low-Ca pyroxenes were not established during thermal metamorphism, but due to the pre-metamorphic differences in low-Ca pyroxene. If this has occurred, materials generated in the nebula differing in conditions of low-Ca pyroxene crystallization have accreted onto the different locality of the parent body.

Acknowledgments

We are grateful to Prof. M. Miyamoto for helpful discussions. Drs. A. Rubin, R. Hutchison and an anonymous referee kindly reviewed the manuscript. This work was partly supported by the Sasagawa Scientific Research Grant from the Japan Science Society.

References

Ashworth, J.R. (1977): Matrix textures in unequilibrated ordinary chondrites. Earth Planet. Sci. Lett., **35**, 25–34.

Bennett, M.E., III and McSween, H.Y., Jr. (1996): Revised model calculations for the thermal histories of ordinary chondrite parent body. Meteoritics, **31**, 783–792.

Binns, R.A. (1967): Structure and evolution of non-carbonaceous chondritic meteorites. Earth Planet. Sci. Lett., **2**, 23–28.

Binns, R.A. (1968): Cognate xenoliths in chondritic meteorites: Examples in Mezö-Madaras and Ghubara. Geochim. Cosmochim. Acta, **32**, 299–317.

Bischoff, A., Geiger, T., Palme, H., Spettel, B., Schultz, L., Scherer, P., Schluter, J. and Lkhamsuren, J.

(1993): Mineralogy, chemistry, and noble gas contents of Adzhi-Bogdo—an LL3-6 chondritic breccia with L-chondritic and granitoidal clasts. Meteoritics, **28**, 570–578.

Brady, J.B. (1995): Diffusion data for silicate minerals, glasses, and liquids. Mineral Physics and Crystallography: A Handbook of Physical Constants, ed. by T.J. Ahrens. Washington, Am. Geophys. Union, 269–290.

Brady, J.B. and McCallister, R.H. (1983): Diffusion data for clinopyroxenes from homogenization and self-diffusion experiments. Am. Mineral., **68**, 95–105.

Brearley, A.J. and Jones, R.H. (1998): Chondritic meteorites. Planetary Materials, ed. by J.J. Papike. Washington, D.C., Mineral. Soc. Am., 3-1 to 3-398.

Bunch, T.E. and Rajan, R.S. (1988): Meteorite regolithic breccias. Meteorites and the Early Solar System, ed. by J.F. Kerridge and M.S. Matthews. Tucson, Univ. Ariz. Press, 144–164.

Carpenter, M.A. (1981): Time-Temerature-Transformation (TTT) analysis of cation disordering in omphacite. Contrib. Mineral. Petrol., **78**, 433–440.

Dodd, R.T. (1981): Meteorites: A Chemical-petrologic Synthesis. Cambridge, Cambridge Univ. Press, 368 p.

Dodd, R.T., Jr., Van Schmus, W.R. and Koffman, D.M. (1967): A survey of the unequilibrated ordinary chondrites. Geochim. Cosmochim. Acta, **31**, 921–951.

Ebihara, M. (1989): Rare earth and some other element in acid-residues of unequilibrated ordinary chondrites. Proc. NIPR Symp. Antarct. Meteorites, **2**, 279–287.

Fodor, R.V. and Keil, K. (1976): Carbonaceous and non-carbonaceous lithic fragments in Plainview, Texas, chondrite: origin and history. Geochim. Cosmochim. Acta, **40**, 177–189.

Ganguly, J. and Tazzoli, V. (1993): Fe^{2+}-Mg^{2+} interdiffusion in orthopyroxene: Constraints from cation ordering and structural data and implications for cooling rates of meteorites. Lunar Planet. Sci. Conf., **24**, 517–518.

Grimm, R.E. (1985): Penecontemporaneous metamorphism, fragmentation, and reassembly of ordinary chondrite parent bodies. J. Geophys. Res., **90**, 2022–2028.

Heyse, J.V. (1978): The metamorphic history of LL-group ordinary chondrites. Earth Planet. Sci. Lett., **40**, 365–381.

Huss, G.R., Keil, K. and Taylor, G.J. (1981): The matrices of unequilibrated ordinary chondrites: implications for the origin and history of chondrites. Geochim. Cosmochim. Acta, **45**, 33–51.

Huebner, J.S. (1980): Pyroxene phase equilibria at low pressure. Pyroxenes, ed. by C.T. Prewitt. Washington, Mineral. Soc. Am., 213–288.

Jones, R.H. (1990): Petrology and mineralogy of type II, FeO-rich chondrules in Semarkona (LL3.0): Origin by closed-system fractional crystallization, with evidence for supercooling. Geochim. Cosmochim. Acta, **54**, 1785–1802

Jones, R.H. (1994): Petrology of FeO-poor, porphyritic pyroxene chondrules in the Semarkona chondrite. Geochim. Cosmochim. Acta, **58**, 5325–5340.

Jones, R.H. and Scott, E.R.D. (1989): Petrology and thermal history of type IA chondrules in Semarkona (LL3.0) chondrite. Proc. Lunar Planet Sci. Conf., 19th, 523–536.

Keil, K. (1982): Composition and origin of chondritic breccias. Lunar Planet. Inst. Tech. Rep., **82-02**, 65–83.

Keil, K., Stöffler, D., Love, S.G. and Scott, E.R.D. (1997): Constraints on the role of impact heating and melting in asteroids. Meteorit. Planet. Sci., **32**, 349–363.

King, V.V., Score, R., Gavel, E.V. and Mason, B. (1980): Meteorite description, in "Catalog of Antarctic Meteorites, 1977–1978". Smithson. Contrib. Earth Sci., **23**, 12–44.

Lee, T., Papanastassiou, D.A. and Wasserburg G.J. (1976) Demonstration of ^{26}Mg excess in Allende and evidence for ^{26}Al. Geophys. Res. Lett., **3**, 109–112.

McCoy, T.J., Scott, E.R.D., Jones, R.H., Keil, K. and Taylor, G.J. (1991): Composition of chondrule silicates in LL3–5 chondrites and implications for their nebular history and parent body metamorphism. Geochim. Cosmochim. Acta, **55**, 601–619.

McSween, H.Y., Jr. and Patchen, A.D. (1989): Pyroxene thermometry in LL-group chondrites and implications for parent body metamorphism. Meteoritics, **24**, 219–226.

McSween, H.Y., Jr., Sears D.W.G. and Dodd, R.T. (1988): Thermal metamorphism. Meteorites and Early Solar System, ed. by J.F. Kerridge and M.S. Matthews. Tucson, Univ. Ariz. Press, 102–113.

Mittlefehldt, D.W. and Lindstrom, M.M. (2001): Petrology and geochemistry of Patuxent Range 91501, a clast-poor impact-melt from the L chondrite parent body and Lewis Cliff 88663, an L7 chondrite.

Meteorit. Planet. Sci., **36**, 439–457.
Miyamoto, M., Fujii, N. and Takeda, H. (1981): Ordinary chondrite parent body: An internal heating model. Proc. Lunar Planet Sci. Conf., 12B, 1145–1152.
Nautiyal, C.M., Padia, J.T., Rao, M.N. Venkatesan, T.R. and Goswami, J.N. (1982): Irradiation history of Antarctic gas-rich meteorites. Lunar and Planetary Science XIII. Houston, Lunar Planet. Inst., 578–579.
Noguchi, T. (1989): Texture and chemical composition of pyroxenes in chondrules in carbonaceous and unequilibrated ordinary chondrites. Proc. NIPR Symp. Antarct. Meteorites, **2**, 169–199.
Noonan, A. F. and Nelen, S. (1976): A petrographic and mineral chemistry study of the Weston, Connecticut, chondrite. Meteoritics, **11**, 111–130.
Rubin, A.E. (1990): Kamacite and olivine in ordinary chondrites: Intergroup and intragroup relationships. Geochim. Cosmochim. Acta, **54**, 1217–1232.
Rubin, A.E. (1995): Petrologic evidence for collisional heating of chondritic asteroids. Icarus, **113**, 156–167.
Rubin, A.E., Scott, E.R.D., Taylor, G.J., Keil, K. and Allen, J.S.B. (1983): Nature of the H chondrite parent body regolith: Evidence from the Dimmit breccia. Proc. Lunar Planet. Sci. Conf., 13th, pt. 2, A741–A754 (J. Geophys. Res., **88**, Suppl.).
Sautter, V., Jaoul, O. and Abel, F. (1988): Aluminum diffusion in diopside using the $^{27}Al(p, \gamma)^{28}Si$ nuclear reaction: preliminary results. Earth Planet. Sci. Lett., **89**, 109–114.
Score, R., King, T.V.V., Schwarz, C.M., Mason, B., Bogard, D.D. and Gabel, E.M. (1981): Antarctic meteorite discriptions 1976–1977–1978–1979. Antarct. Meteorite Newsl., **4** (1), 144 p.
Scott, E.R.D. (1984): Classification, metamorphism, and brecciation of type-3 chondrites from Antarctica. Smithson. Contrib. Earth Sci., **26**, 73–94.
Scott, E.R.D. and Rajan, R.S. (1981): Metallic minerals, thermal histories and parent bodies of some xenolithic, ordinary chondrite meteorites. Geochim. Cosmochim. Acta, **45**, 53–67.
Scott, E.R.D., Taylor, G.J., Rubin, A.E., Okada, A. and Keil, K. (1981a): Graphite-magnetite aggregates in ordinary chondritic meteorites. Nature, **291**, 544–546.
Scott, E.R.D., Taylor, G.J., Rubin, A.E. and Keil, K. (1981b): New kind of type 3 chondrite with a graphite-magnetite matrix. Earth Planet. Sci. Lett., **56**, 19–31.
Scott, E.R.D., Lusby, D. and Keil, K. (1985): Ubiquitous brecciation after metamorphism in equilibrated ordinary chondrites. Proc. Lunar Planet. Sci. Conf., 16th, pt. 1, D137–D148 (J. Geophys. Res., **90**, Suppl.).
Sears, D.W.G., Hasan, F.A., Batchelor, J.D. and Lu, J. (1991): Chemical and physical studies of type 3 chondrites—XI: Metamorphism, pairing, and brecciation of ordinary chondrites. Proc. Lunar Planet. Sci., **21**, 493–512.
Stöffler, D., Keil, K. and Scott, E.R.D. (1991): Shock metamorphism of ordinary chondrites. Geochim. Cosmochim. Acta, **55**, 3845–3867.
Taylor, G.J., Maggiore, P., Scott, E.R.D., Rubin, A.E. and Keil, K. (1987): Original structures, and fragmentation and reassembly histories of asteroids: Evidence from meteorites. Icarus, **69**, 1–13.
Tsuchiyama, A., Fujita, T. and Morimoto, N. (1988): Fe-Mg heterogeneity in the low-Ca pyroxenes during metamorphism of the ordinary chondrites. Proc. NIPR Symp. Antarct. Meteorites, **1**, 173–184.
Van Schmus, W.R. and Wood, J.A. (1967): A chemical-petrologic classification for the chondritic meteorites. Geochim. Cosmochim. Acta, **31**, 747–765.
Wasson, J. T. (1974): Meteorites: Classification and Properties. Berlin, Springer, 316 p.
Yanai, K. and Kojima, H., comp. (1987): Photographic Catalog of the Antarctic Meteorites. Tokyo, Natl. Inst. Polar Res., 298 p.

(Received December 8, 2001; Revised manuscript accepted January 29, 2002)